First results from the PHOBOS spectrometer

Nigel George for the PHOBOS Collaboration
B.B.Back[1], M.D.Baker[2], D.S.Barton[2], R.R.Betts[1,6], R.Bindel[7], A.Budzanowski[3], W.Busza[4], A.Carroll[2], M.P.Decowski[4], E.Garcia[7], N.George[1], K.Gulbrandsen[4], S.Gushue[2], C.Halliwell[6], J.Hamblen[8], G.A.Heintzelman[2], C.Henderson[4], R.Hołyński[3], D.J.Hofman[6], B.Holzman[6], E.Johnson[8], J.L.Kane[4], J.Katzy[4], N. Khan[8], W.Kucewicz[6], P.Kulinich[4], W.T.Lin[5], S.Manly[8], D.McLeod[6], J.Michałowski[3], A.C.Mignerey[7], J.Mülmenstädt[4],R.Nouicer[6], A.Olszewski[2,3], R.Pak[2], I.C.Park[8], H.Pernegger[4], C.Reed[4], L.P.Remsberg[2], M.Reuter[6], C.Roland[4], G.Roland[4], L.Rosenberg[4], P.Sarin[4], P.Sawicki[3], W.Skulski[8], S.G.Steadman[4], G.S.F.Stephans[4], P.Steinberg[2], M.Stodulski[3], A.Sukhanov[2], J.-L.Tang[5], R.Teng[8], A.Trzupek[3], C.Vale[4], G.J.van Nieuwenhuizen[4], R.Verdier[4], B.Wadsworth[4], F.L.H.Wolfs[8], B.Wosiek[3], K.Woźniak[3], A.H.Wuosmaa[1], B.Wysłouch[4]

[1] Argonne National Laboratory, [2] Brookhaven National Laboratory, [3] Institute of Nuclear Physics, Kraków, Poland [4] Massachusetts Institute of Technology, [5] National Central University, Chung-Li, Taiwan [6] University of Illinois at Chicago, [7] University of Maryland, [8] University of Rochester

The ratios of antiparticle to particle production in central Au+Au collisions at $\sqrt{s_{NN}} =$ 130 GeV within the rapidity range 0.2 < y < 0.9 are presented. The measurement was made using the PHOBOS spectrometer at RHIC with a p_t acceptance for identified particles of $0.1 < \mathrm{p_t} < 1.1$ GeV/c. Excellent background rejection was achieved by high resolution tracking within 10 cm of the collision point. Inferences regarding the chemical freeze-out environment and model comparisons are made.

1. Introduction

The Relativistic Heavy-Ion Collider(RHIC) at Brookhaven National Laboratory successfully delivered heavy-ion collisions at the highest center-of-mass energies ever achieved in the laboratory in the summer of 2000. Such collisions allow the study of the fundamental properties of nuclear matter under high particle and energy densities.

Aside from the “first look” potential of any measurement from these collisions, particle ratios can provide important information on the hadro-chemical environment of the collision [1]. Baryonic ratios also provide information on baryon transport within these collisions [2].

In this paper we present the measured ratios of charged antiparticles to particles for pions, kaons and protons. These measurements were made in the PHOBOS spectrometer near mid-rapidity for the 12% most central inelastic Au+Au collisions with $\sqrt{s_{NN}} =$ 130 GeV. Inferences on baryon transport will be presented and chemical potentials are extracted.

2. Tracking and Particle Identification in the PHOBOS spectrometer

The PHOBOS spectrometer[3] has a horizontal bending plane with an overall range of acceptance of $\sim 5^o$ in azimuth and $\sim 66^o$ in polar angle relative to the beam direction. Eight tracking layers are located between the collision point and the magnetic field region. Within the magnetic field region(2T) there are an additional eight tracking layers. Thus the direction and momentum of tracks can be determined. The tracking layers consist of highly segmented, $\leq$ 1mm in the bend direction, silicon pads. The pads define the position and specific ionization($\frac{\mathrm{dE}}{\mathrm{dx}}$) of track hits in a layer.

Tracks are reconstructed in the spectrometer using the following algorithm: In the first six layers, clusters of hits in (θ, ϕ) define straight-line track segments. The common intersection point of these segments determines the vertex position ($\sigma_x = 450\ \mu$m, $\sigma_y = \sigma_z = 200\ \mu$m). In the field region, pairs of hits are tranformed into pairs of track momentum and polar angle $(\frac{1}{p}, \theta)$, using the found vertex. Clusters in $(\frac{1}{p}, \theta)$ define the curved part of the track. The curved track segments thus found are matched to the straight-line parts using geometric and $\frac{\mathrm{dE}}{\mathrm{dx}}$(truncated mean) matching criteria. Finally, a cut on the distance of closest approach to the vertex is made ($\mathrm{dca_{vtx}} < 3.5$ mm).

Figure 1 shows the resulting track $\frac{\mathrm{dE}}{\mathrm{dx}}$ vs p distribution, with the particle identification regions outlined. Within these regions we are able to identify pions up to a total momenta of 0.6 GeV/c, kaons up to 0.75 GeV/c and protons up to 1.1 GeV/c.

3. Antiparticle to particle ratio determination

The analyzed data were taken with the two polarity settings, B=+1 and B=-1. Off-line event centrality selections were made using signals from scintillator counters on either side of the collision region, for details see [4,5]. The analysis performed here was done using the 12% $\sigma_{AuAu}^{inelastic}$ most central Au+Au collisions. Using a Glauber-type calculation[5] the average number of participants is estimated to be about 310 for the selected events.

To optimize the vertex precision and track-finding performance, only events with vertices in the range -15 cm $< \mathrm{z_{vtx}} < 9$ cm were used. Due to the limited acceptance of the spectrometer the kinematic coverage is highly vertex dependent. For vertices in the given range, the kinematic coverage over which the ratios are determined is shown in Figure 2.

For each species, the ratio is determined by the measured number of antiparticles per event with a particular field polarity setting divided by the measured number of particles per event obtained with the opposite field polarity setting. In this way, track reconstruction efficiencies and acceptances cancel, significantly reducing the overall systematic uncertainty. Since the spectrometer accepts both positive and negative charge states of each particle type at each field setting, the particle ratios are determined from the average of the antiparticle to particle ratios obtained with both field combinations. This ratio is then corrected for the effects of different contributions to the measured number of antiparticle and particle tracks. Equation 1 shows the resulting expression for calculating the final antiparticle to particle ratio.

$$\frac{\overline{\mathrm{Part}}}{\mathrm{Part}} = \frac{\left\langle E\frac{dN}{dp^3}\right\rangle_{\overline{Part}}}{\left\langle E\frac{dN}{dp^3}\right\rangle_{\mathrm{Part}}} = \frac{1}{2}\left(\frac{n_{B=+1}^{\overline{\mathrm{Part}}}}{n_{B=-1}^{\mathrm{Part}}} + \frac{n_{B=-1}^{\overline{\mathrm{Part}}}}{n_{B=+1}^{\mathrm{Part}}}\right) \times \mathrm{C_{Absorption}} \times \mathrm{C_{WeakDecay}} \times \mathrm{C_{Secondaries}} \qquad (1)$$

where n is the measured number of (anti)particles per event, for a given field polarity.

The dominant correction to the baryon ratio($\frac{\overline{\mathrm{p}}}{\mathrm{p}}$) arises from the higher absorption cross

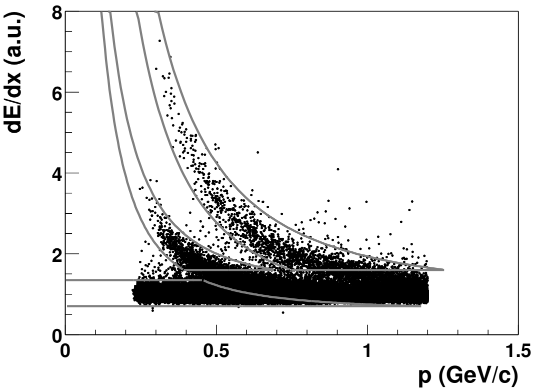

Figure 1. Distribution of the truncated energy loss average, in arbitary units (a.u.), as a function of the reconstructed particle momentum. Three clear bands can be seen, corresponding to pions, kaons and protons. The solid lines indicate the cut regions for counting identified particles.

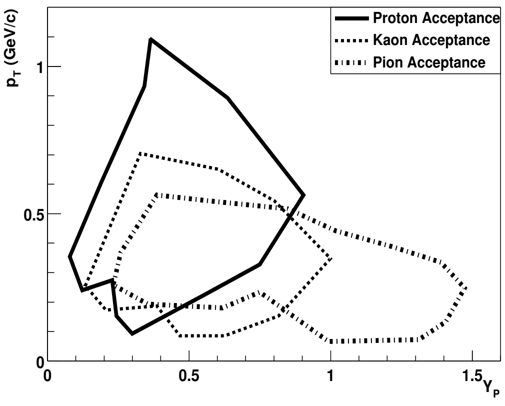

Figure 2. Acceptance of the spectrometer as a function of p_t and rapidity for pions, kaons and protons. The acceptance is averaged over the accepted vertex range and both field polarity settings.

section in material for antiprotons. This correction is p_t dependent, and ranges from 7% at $p_t = 150\ MeV/c$ to 3% at $p_t = 900\ MeV/c$. The baryon ratio correction due to contamination of the ratio from weak hyperon decays with different antiparticle to particle ratios(e.g. $\Lambda \rightarrow p\pi^-, \overline{\Lambda} \rightarrow \overline{p}\pi^+$) is found to be 2% and independent of p_t. A good weak decay product rejection($> 50\%$) is obtained due to tracking within 10 cm of the collision point. The final baryon ratio correction is due to more protons than antiprotons being produced from secondary interactions, predominantly in the beam pipe. This correction is p_t dependent and ranges from 5% at $p_t = 150\ MeV/c$ to negligible beyond $p_t = 500\ MeV/c$. The correction factors for pions and kaons are negligible.

4. Results and Discussion

Applying the above corrections, the following preliminary antiparticle to particle ratios within our acceptance for the 12% most central collisions are: $\frac{\langle\pi^-\rangle}{\langle\pi^+\rangle} = 1.01 \pm 0.01(\text{stat.}) \pm 0.05(\text{syst.})$, $\frac{\langle K^-\rangle}{\langle K^+\rangle} = 0.91 \pm 0.09(\text{stat.}) \pm 0.1(\text{syst.})$ and $\frac{\langle\overline{p}\rangle}{\langle p\rangle} = 0.54 \pm 0.05(\text{stat.}) \pm 0.1(\text{syst.})$.

There are two contributions to the quoted systematic uncertainties, one from the estimation of the correction factors and the other from the determination of the uncorrected ratios. The latter contribution is estimated from the difference between the antiparticle to particle ratios found using both field polarity configurations.

The center of mass energy dependence of the $\frac{\mathrm{K}^-}{\mathrm{K}^+}$ and $\frac{\overline{\mathrm{p}}}{\mathrm{p}}$ ratios is shown in Figure 3.

An overall excess of protons over antiprotons in the mid-rapidity region is implied from the measured $\frac{\overline{\mathrm{p}}}{\mathrm{p}}$ ratio. From isospin symmetry arguments, a similar excess of neutrons over antineutrons can be expected. Assuming a quark coalecence model, $\frac{\langle\overline{\Lambda}\rangle}{\langle\Lambda\rangle} = \frac{\langle K^+\rangle}{\langle K^-\rangle} \cdot \frac{\langle\overline{p}\rangle}{\langle p\rangle}$, a similar excess of hyperons over antihyperons is expected. These are the dominant carriers of baryon number at mid-rapidity. Hence, one can infer that there is a non-zero net baryon density in the mid-rapidity region in central Au+Au collisions at such high energy.

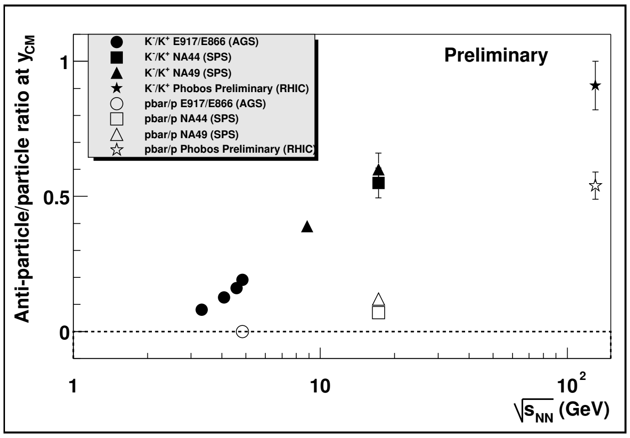

Figure 3. Mid-rapidity $\frac{\mathrm{K}^-}{\mathrm{K}^+}$ and $\frac{\overline{\mathrm{p}}}{\mathrm{p}}$ ratios for central Au+Au collisions as a function of the center of mass energy per nucleon pair. The $\frac{\mathrm{K}^-}{\mathrm{K}^+}$ ratios are represented by the filled symbols. The $\frac{\overline{\mathrm{p}}}{\mathrm{p}}$ ratios are represented by the open symbols. The quoted results of other experiments are from these proceedings and Nucl. Phys. A661 (1999)

It is interesting to note that the measured $\frac{\overline{\mathrm{p}}}{\mathrm{p}}$ ratio, $0.54 \pm 0.05(\mathrm{stat.}) \pm 0.1(\mathrm{syst.})$, falls in between models with different amounts of stopping: HIJING, a model with little stopping, predicts 0.77 [6], while RQMD, a model with significant stopping, predicts 0.42 [7].

From the measured ratios, the chemical freeze-out parameters can be deduced, using a simple thermodynamic model[8] (i.e. $\left.\frac{dN}{dp^3}\right|_p / \left.\frac{dN}{dp^3}\right|_{\overline{p}} = \exp\frac{2\mu_B}{kT}$). The $\frac{\overline{p}}{p}$ ratio implies $\frac{\mu_B}{kT} = 0.31 \pm 0.05(\mathrm{stat.})$. Assuming typical chemical freeze-out temperatures between 150-200 MeV, a baryon chemical potential around 50 MeV is estimated. This value is significantly smaller than was observed at the SPS where $\mu_B = 266 \pm 5$ MeV [9]. This chemical potential is consistent with a non-zero net baryon density in the mid-rapidity region. Because of the extreme sensitivity of the expression to particle ratios close to unity only a semi-quantitive statement that $\frac{\mu_S}{kT} \approx 0$ can be made.

An additional model comparison can be made with a thermal model presented by Redlich[10] at this conference. This model predicts the expected $\frac{\mathrm{K}^-}{\mathrm{K}^+}$ ratio as a function of $\frac{\overline{\mathrm{p}}}{\mathrm{p}}$. It was found, using our measured $\frac{\overline{\mathrm{p}}}{\mathrm{p}}$ results, that the predicted $\frac{\mathrm{K}^-}{\mathrm{K}^+}$ of 0.87 agrees with our measured kaon ratio.

Acknowledgements: This work was partially supported by: (US) DoE grants DE-AC02-98CH10886, DE-FG02-93ER40802, DE-FC02-94ER40818, DE-FG02-94ER40865, DE-FG02-99ER41099 and W-31-109-ENG-38, NSF grants 9603486, 9722606 and 0072204, (Poland) KBN grant 2 P03B 04916, (Taiwan) NSC contract NSC 89-2112-M-008-024.

REFERENCES

1. J. Letessier *et al.*, Phys. Rev. **D51** (1995) 3408.
2. S.E. Vance, Nucl. Phys. **A661**, (1999)230c.
3. R. Pak, PHOBOS Collaboration, these proceedings.
4. J. Katzy, PHOBOS Collaboration, these proceedings.
5. B. Back *et al.*, Phys. Rev. Lett. **85** (2000) 3100.
6. M.Gyulassy and X.N.Wang, Phys. Rev. **D44** (1991) 3501. We used HIJING V1.35 (April 1998) with standard parameter settings.
7. H. Sorge *et al.* Ann. Phys. **192** (1989) 266
8. A.Z. Mekjian, Phys. Rev. Lett. **38** (1977) 640.
9. P. Braun-Munzinger, I. Heppe, J. Stachel, Phys. Lett. **B465** (1999) 15.
10. K. Redlich *et al.*, these proceedings.